Strain Sensing Ability of Metallic Particulate Reinforced Cementitious Composites: Experiments and Modeling

Avinaya Tripathi

Pu Yang

Narayanan Neithalath

School of Sustainable Engineering and the Built Environment

Arizona State University

Narayanan.Neithalath@asu.edu;
http://neithalath.engineering.asu.edu

Presented at the ACI Fall 2023 Convention, November 1, 2023

Sustainability of cement-based materials

- Concrete industry always in search of cement replacement materials
  - Environmental and energy impacts of cement production
  - Resource conservation
- Cement Sustainability Initiative
  - Fuel efficiency
  - Process emissions
  - Clinker reduction
  - CCS

Shan et al. 2019

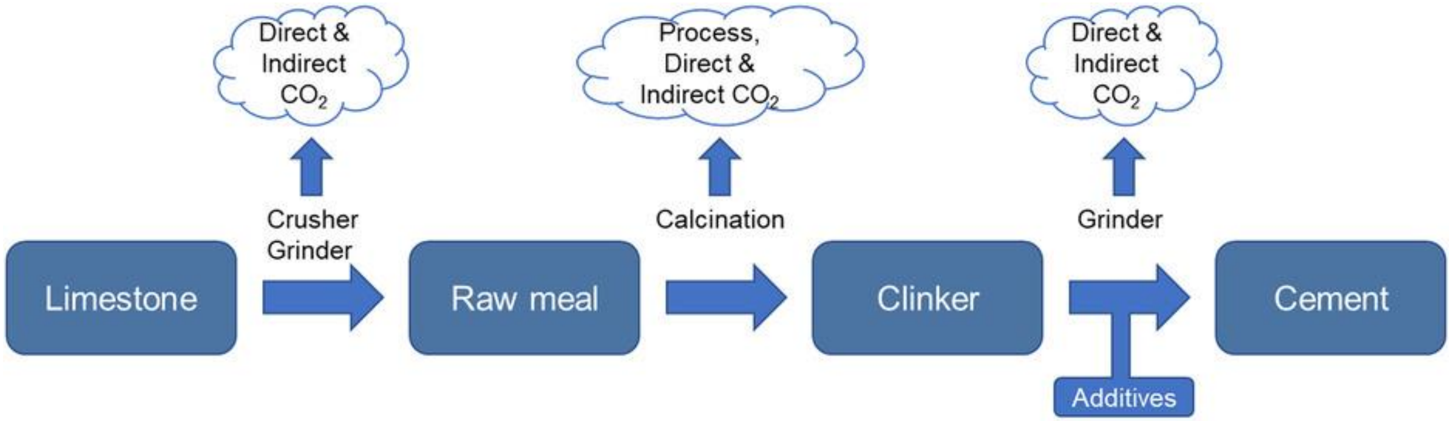

Metallic iron powder waste

- During manufacturing of steel, a significant amount of baghouse dust is produced
- Typically extracted by the air pollution control system on an Electric Arc Furnace (EAF)
- Steel plant waste is difficult to recycle back : not economically feasible
- Traditional means of disposing EAF dust is landfilling - cost varies from country to country



Presented at the ACI Fall 2023 Convention, November 1, 2023

Metallic carbonation

- One method to form carbon-negative binders

$$Fe + 2CO_2 + 2H_2O \rightarrow Fe^{2+} + 2HCO_3^- + H_2 \uparrow$$

$$Fe^{2+} + 2HCO_3^- \rightarrow FeCO_3 + CO_2 + H_2O$$

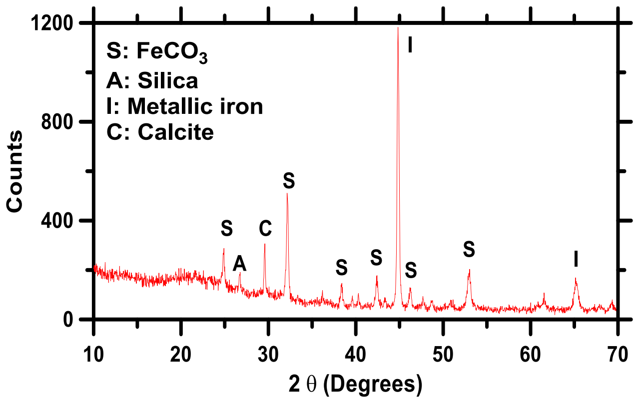

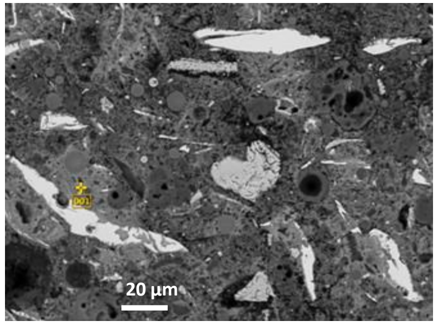

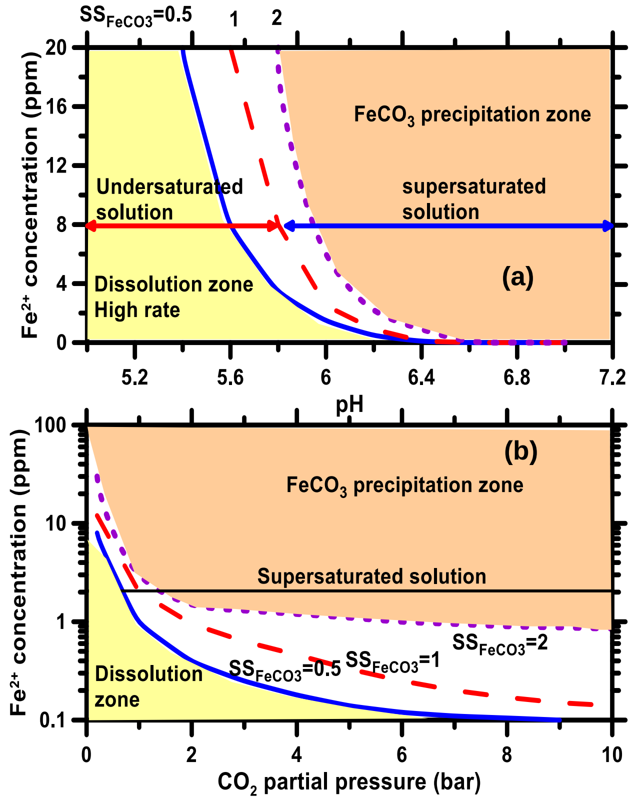

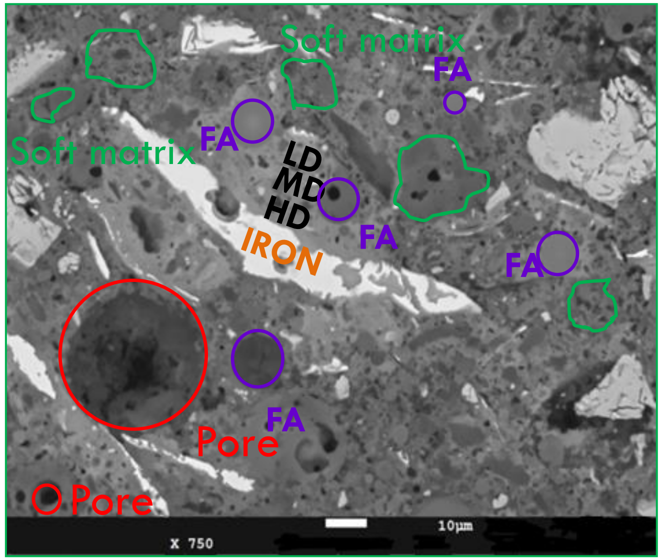

Metallic powder in conventional binders

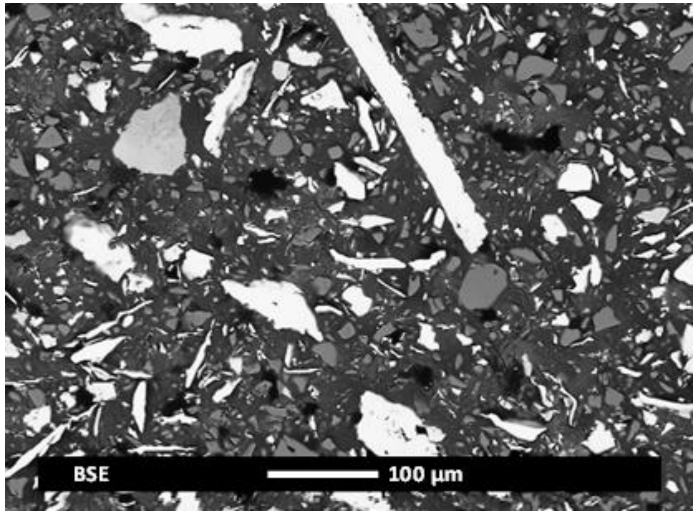

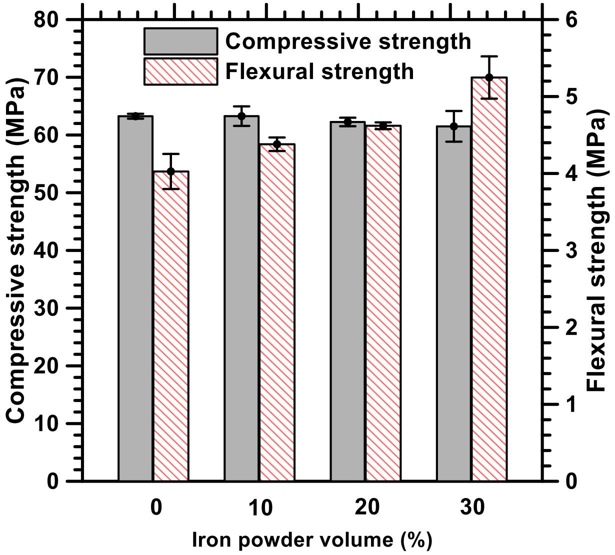

Alkali activated slag – iron powder matrix

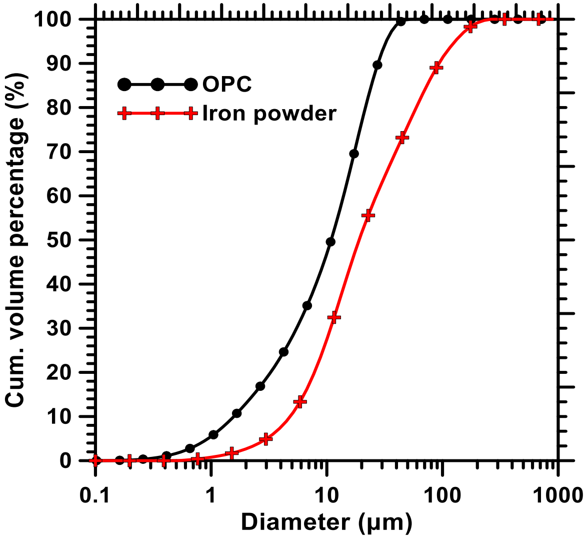

OPC-iron powder matrix

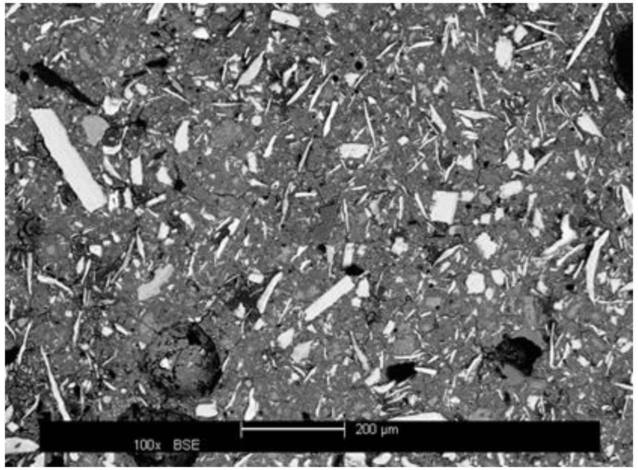

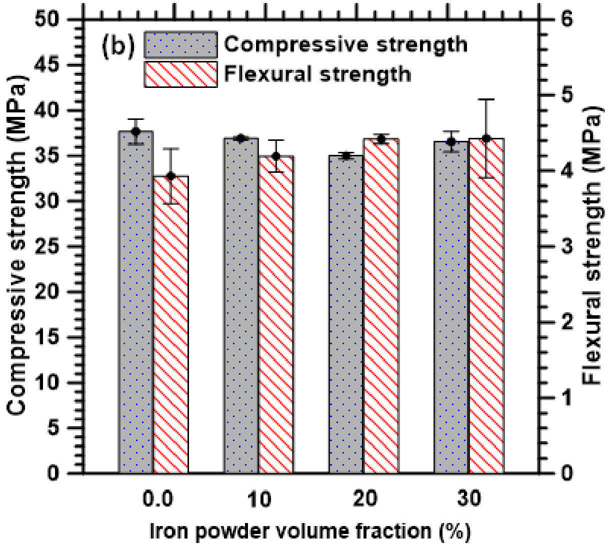

Experiments

- 0-40% by volume of iron powder replacing cement

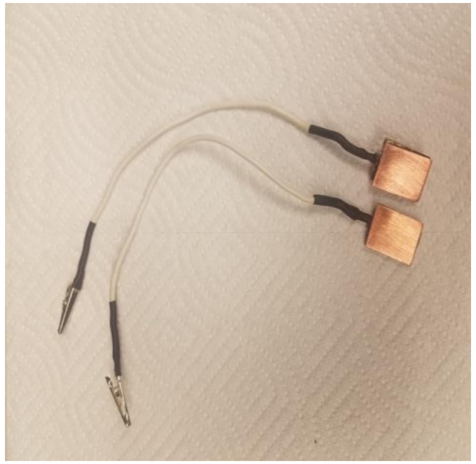

Copper electrodes

Beam with electrodes

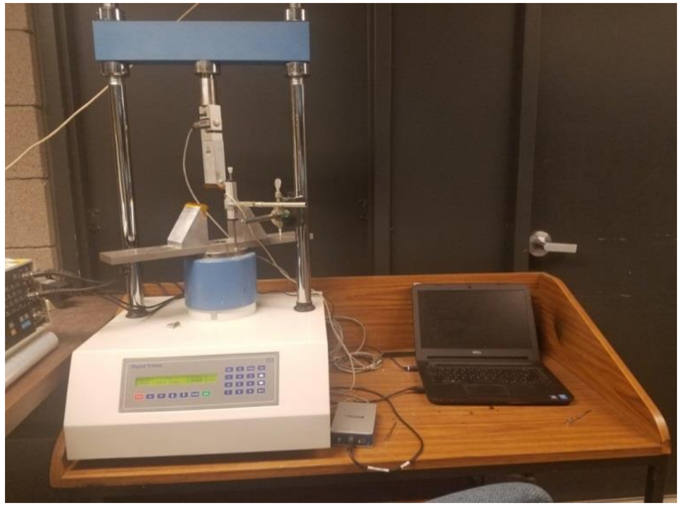

Loading system connected to impedance spectroscope

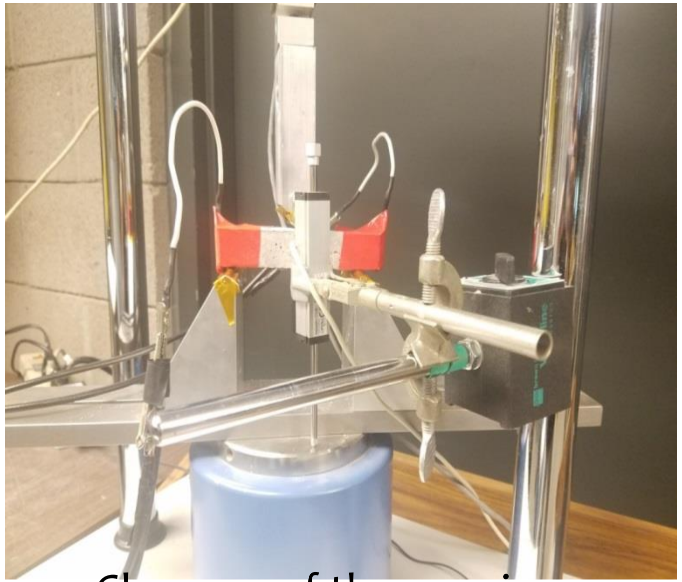

Close up of the specimen under test

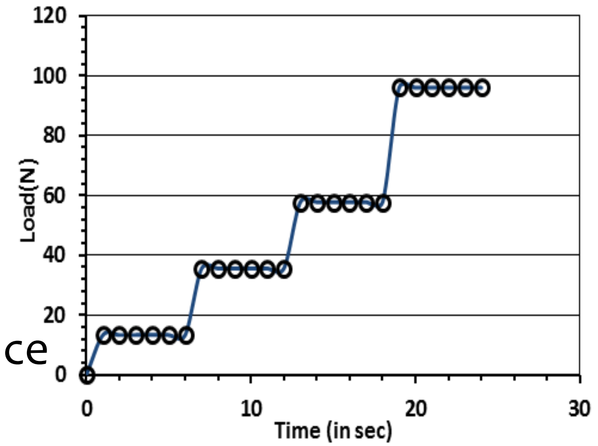

Loading sequence

Electrical response

- Frequency-dependent AC measurements
- Accurate determination of the bulk resistance requires such measurements - cut-off frequency has been reported to vary over two orders of magnitude
- Little change in the Nyquist plots of OPC pastes with loading, indicating that it has little-to-no capacity to self-sense strain
- Presence of metallic particulate reinforcement decreases the overall resistance of the composite

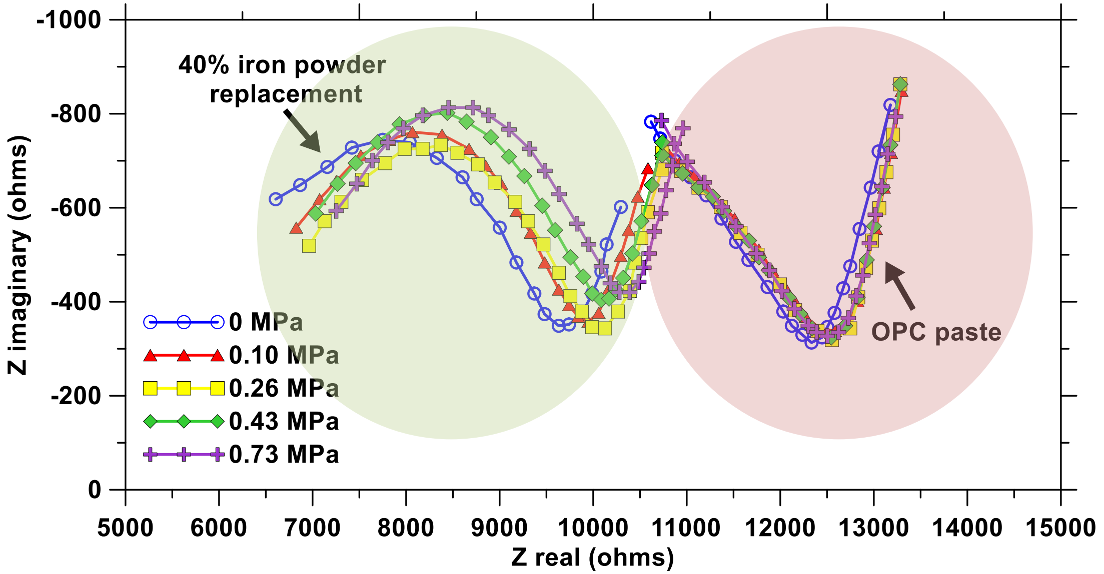

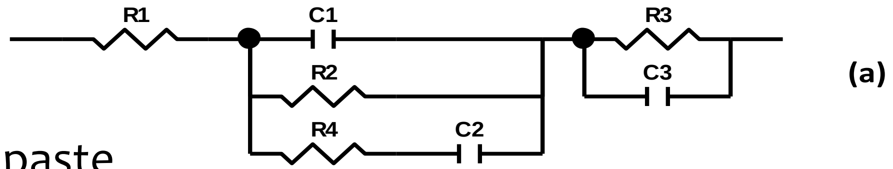

OPC paste

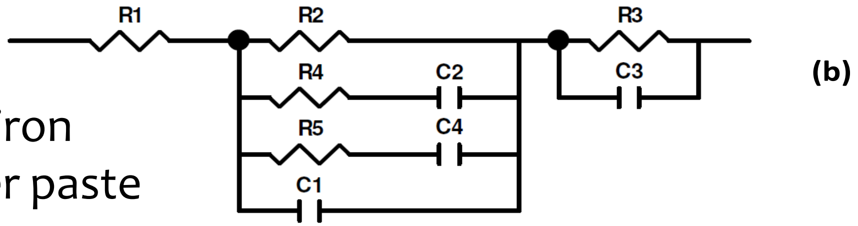

OPC + iron powder paste

Some considerations

- Volume fractions of conductive particulates considered to be generally above the 3D percolation threshold
- Above the percolation threshold, sensing is more sensitive to tension than to compression
- Tension separates the conducting network – increase in resistance with increasing tensile stress (load).
- When the impedance of the whole sample is measured (in lieu of resistance being just measured on the tension or compression sides of a beam undergoing flexure), the response is in line with what would be expected under tension.
- Safe to consider that the electrical response is collected during a tensile event – used in simulations

Equivalent circuits

- Resistance of the connected pores (R_2) is considered as the bulk resistance (R_b) of the sample for the plain cement paste
- For matrices containing iron powder, bulk resistance is taken as the equivalent resistance of the connected pores (R2) and iron particles (R5) in parallel
- R_b values obtained using both the methods differ by 5-10%.

OPC paste

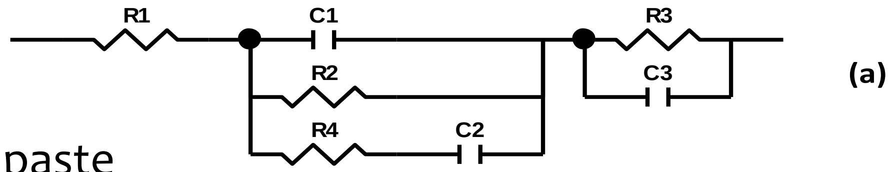

OPC + iron powder paste

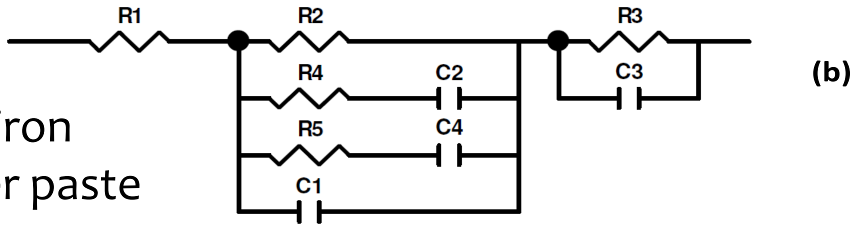

- R1 - electrode resistance
- R2 - resistance of connected pores
- R3 - resistance offered by the conducting medium between the electrode and the sample
- R4 - resistance attributed to unconnected or isolated pores
- C1 - capacitance related to the interface of solid phases
- C2 - capacitance associated with the interface between pore wall and bulk pore solution
- R5 and C4 - resistance of the iron particulates and capacitance between iron powder and bulk solid respectively

Fractional change in resistance

- Fractional change in resistance ($\Delta R/R_o$) corresponding to each stress level
- ΔR denotes the difference between the measured bulk resistance at a given stress level and the bulk resistance before loading
- Tests done on non-dried samples
  - Water interferes with the electronic conduction across conductive particle-matrix interface
  - Reported quantifications of self-sensing capabilities of these matrices are conservative.
- Presence of a conductive component amplifies the strain sensing capability

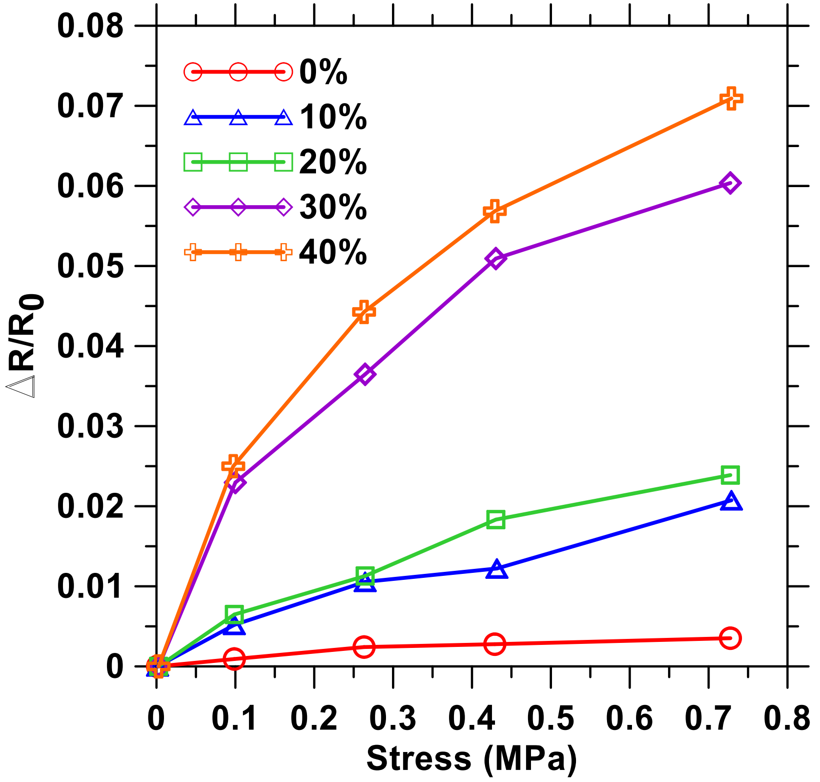

Gage factor

- $\Delta R/R_o$ at iron particulate between 10% and 40% - similar to those obtained for cementitious matrices containing small volume fractions of continuous or discrete carbon fibers
  - Implications with cost
- Gage factor - fractional change in resistance per unit strain
- A useful indicator of the applicability of the sensor
- Comparable values to that of carbon fiber and steel fiber reinforced composites

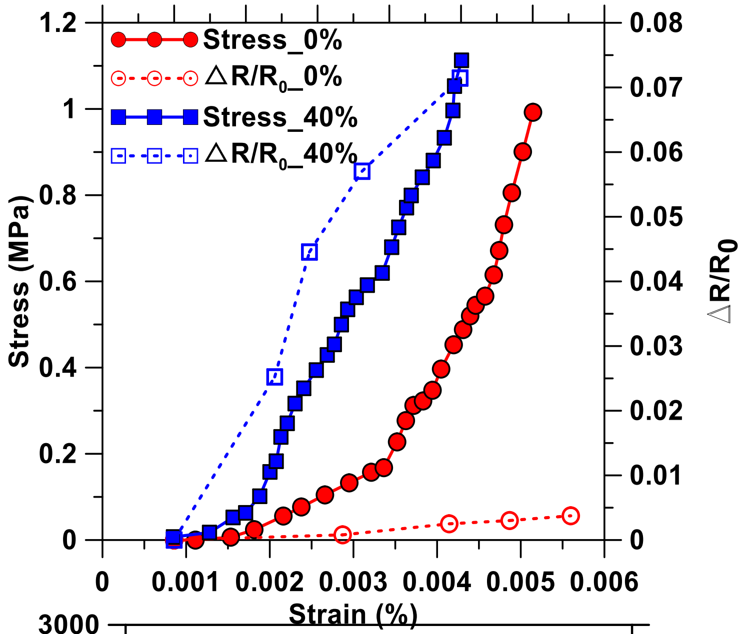

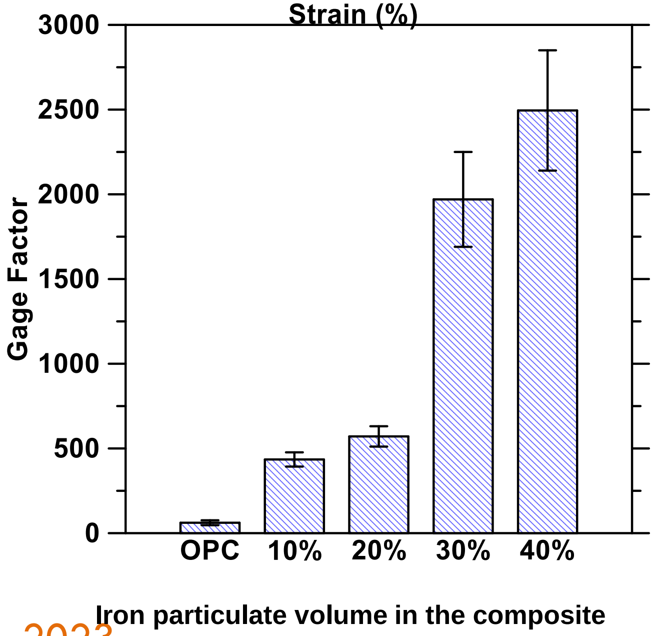

Modeling the strain sensing response

- Considers the mechanical and electrical response
- Heterogeneity of the microstructure makes modeling complex
- Effective properties of the composite are non-linear combinations of the individual properties due to the complex microstructure.
- For the metallic particulate reinforced cementitious system, the microstructure composed of:
  - the host (cement paste/mortar),
  - inclusions (elongated iron particles)
  - interface between the inclusion and the host.

Electrical response of the host

$$\varepsilon_h(\omega) = \varepsilon'(\omega) - j\varepsilon''(\omega) = \frac{1}{j\omega C_0 Z(\omega)}$$

$$\varepsilon'(\omega) - j\varepsilon''(\omega) = \frac{\omega C_0 Z''}{\omega^2 C_0^2 (Z'^2 + Z''^2)} - j\frac{\omega C_0 Z'}{\omega^2 C_0^2 (Z'^2 + Z''^2)}$$

$$Cole - Cole\ fit: \quad \varepsilon(\omega) = \varepsilon_\infty + \frac{\varepsilon_L - \varepsilon_\infty}{(1 + j\omega\tau)^{1-s}}$$

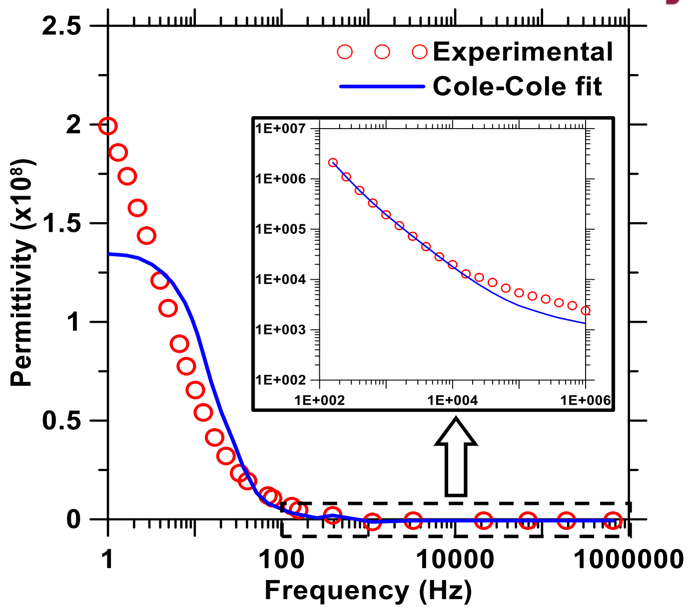

Cole-Cole modification allows for the incorporation of the effects of different phases in a heterogeneous microstructure by using a distribution of time constants, which is accomplished by changing the value of (1-s)

$$\sigma_h(\omega) = \sigma'(\omega) - j\sigma''(\omega) = \frac{Z'Z''\omega}{\omega^2 C_0^2 (Z'^2 + Z''^2)^2} - j\frac{Z'^2\omega}{\omega^2 C_0^2 (Z'^2 + Z''^2)^2}$$

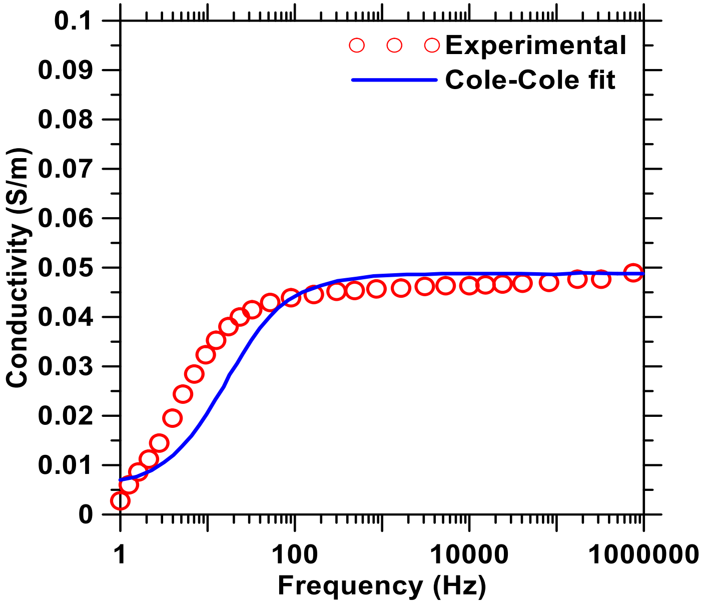

Tarasov-Titov modification of C-C $\quad \sigma(\omega) = \sigma_\infty \left[1 - \frac{m}{1 + (j\omega\tau)^c}\right]$

τ is the time constant and c is a dispersion parameter, taken as 0.02 s and 0.80 respectively

Electrical response of the inclusion

- Conducting particles assumed to be surrounded by an interface of constant thickness
- Inclusion and interface combined into an ‘effective particle’, and embedded in the paste
- With increase in the inclusion volume fraction, only the total number of ‘effective particles’ increase, and the effective properties of the particles remain invariant
- EMT can then be used

$$9(1-\phi_e)\frac{\sigma_1^{\frac{1}{s}}-\sigma_{eff}^{\frac{1}{s}}}{2\sigma_{eff}^{\frac{1}{s}}+\sigma_1^{\frac{1}{s}}}+\phi_e\left(\frac{\sigma_2^{\frac{1}{t}}-\sigma_{eff}^{\frac{1}{t}}}{\sigma_{eff}^{\frac{1}{t}}+A_{21}\left(\sigma_2^{\frac{1}{t}}-\sigma_{eff}^{\frac{1}{t}}\right)}+4\frac{\sigma_2^{\frac{1}{t}}-\sigma_{eff}^{\frac{1}{t}}}{2\sigma_{eff}^{\frac{1}{t}}+(1-A_{21})\left(\sigma_2^{\frac{1}{t}}-\sigma_{eff}^{\frac{1}{t}}\right)}\right)=0$$

$$\phi_e=\frac{\phi}{\eta}$$

$$\eta=\frac{ab^2}{(a+\lambda)(b+\lambda)^2}$$

σ_{eff} is the conductivity of the composite, σ_1 is the conductivity of the cement paste, σ_2 is the conductivity of the effective particle, and ϕ_e is the volume fraction of the effective particles. A_{21} is a depolarization factor, taken as 1/3, s and t are numerical fitting parameters, and λ is the effective thickness of interface

Interface properties

- Equations programmed in MATLAB to back-calculate the interfacial conductivity and permittivity
- Thickness of the interface is taken as 5 μm
- s and τ are obtained as 0.99 and 0.0086 s respectively while for the electrical conductivity fit, m, τ, and c used are 0.99, 0.0086 s, and 0.40 respectively

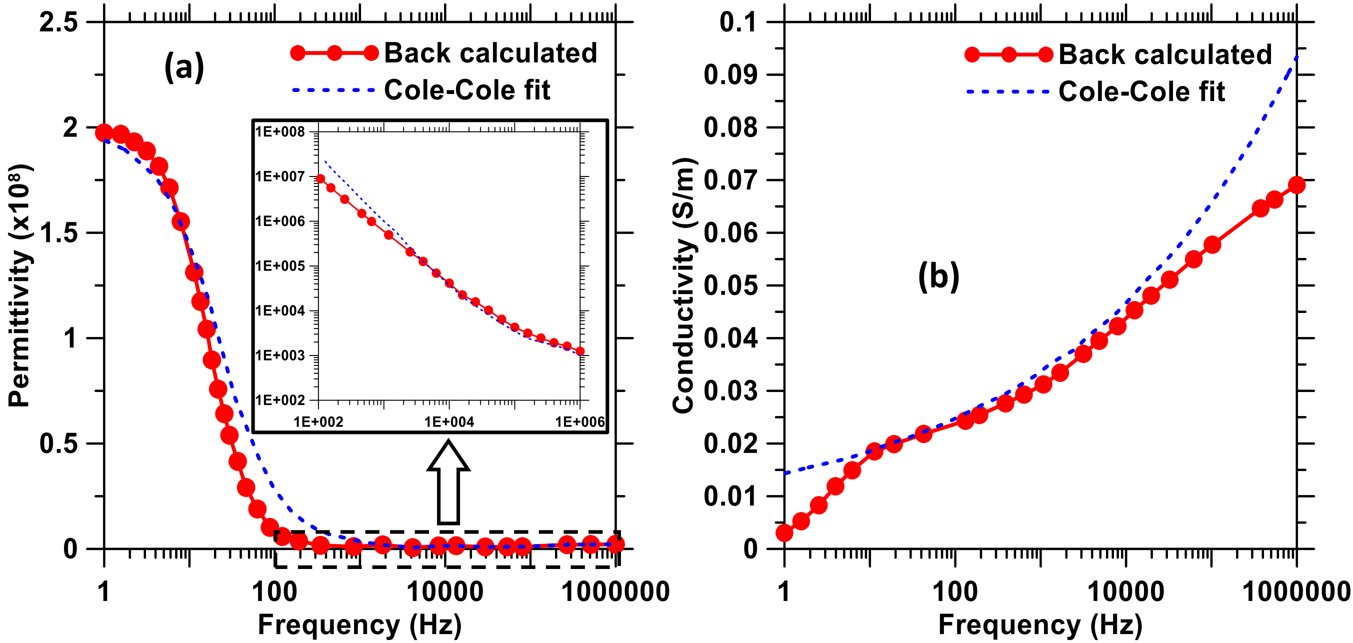

Microstructure generation

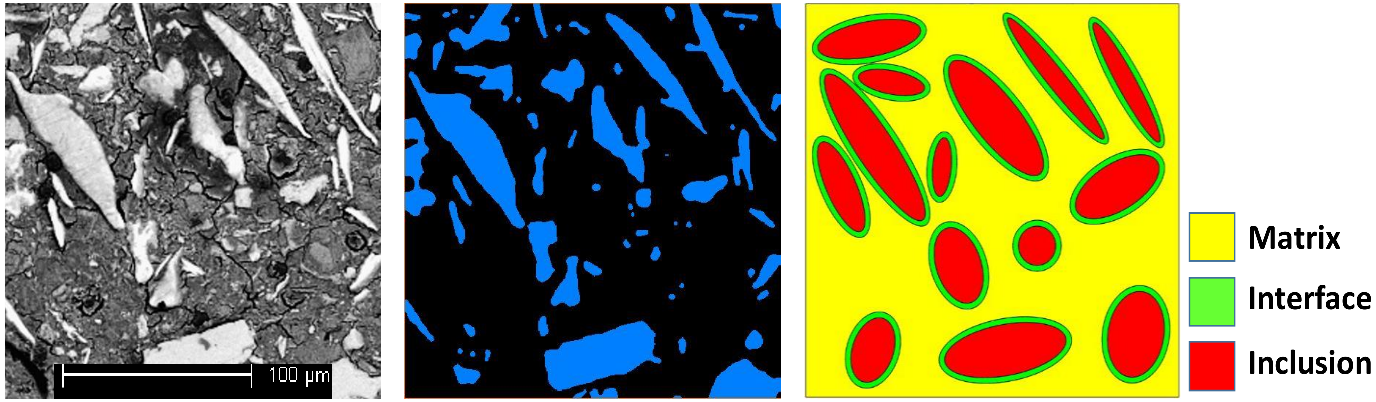

(a) (b) (c)

- All the inclusions replaced with ellipses while maintaining the same volume fraction, locations, and orientations as in the parent micrograph
- Very small inclusions close to one another merged
- Elliptical inclusions circumscribed by elliptical rings of 5 μm thickness for interfaces

Electro-mechanical FE modeling

Arizona State University

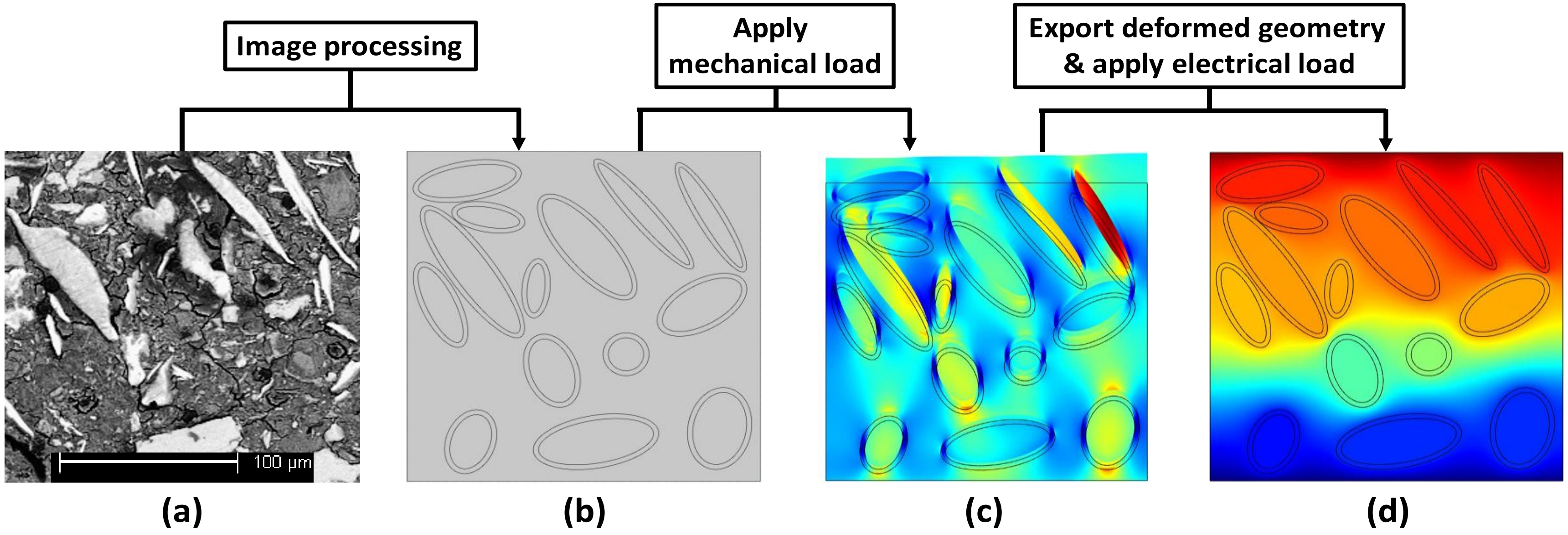

- COMSOL to model the behavior
- Modeling process loosely mirrors the physical process - specimen subjected to a load, and the electrical response under that load measured - to determine strain sensing efficiency

Phase	E (GPa)	ν	ρ (kg/m³)
Matrix	20	0.20	2000
Interface	9	0.26	1500
Inclusion	150	0.40	7850

Electro-mechanical FE modeling

Arizona State University

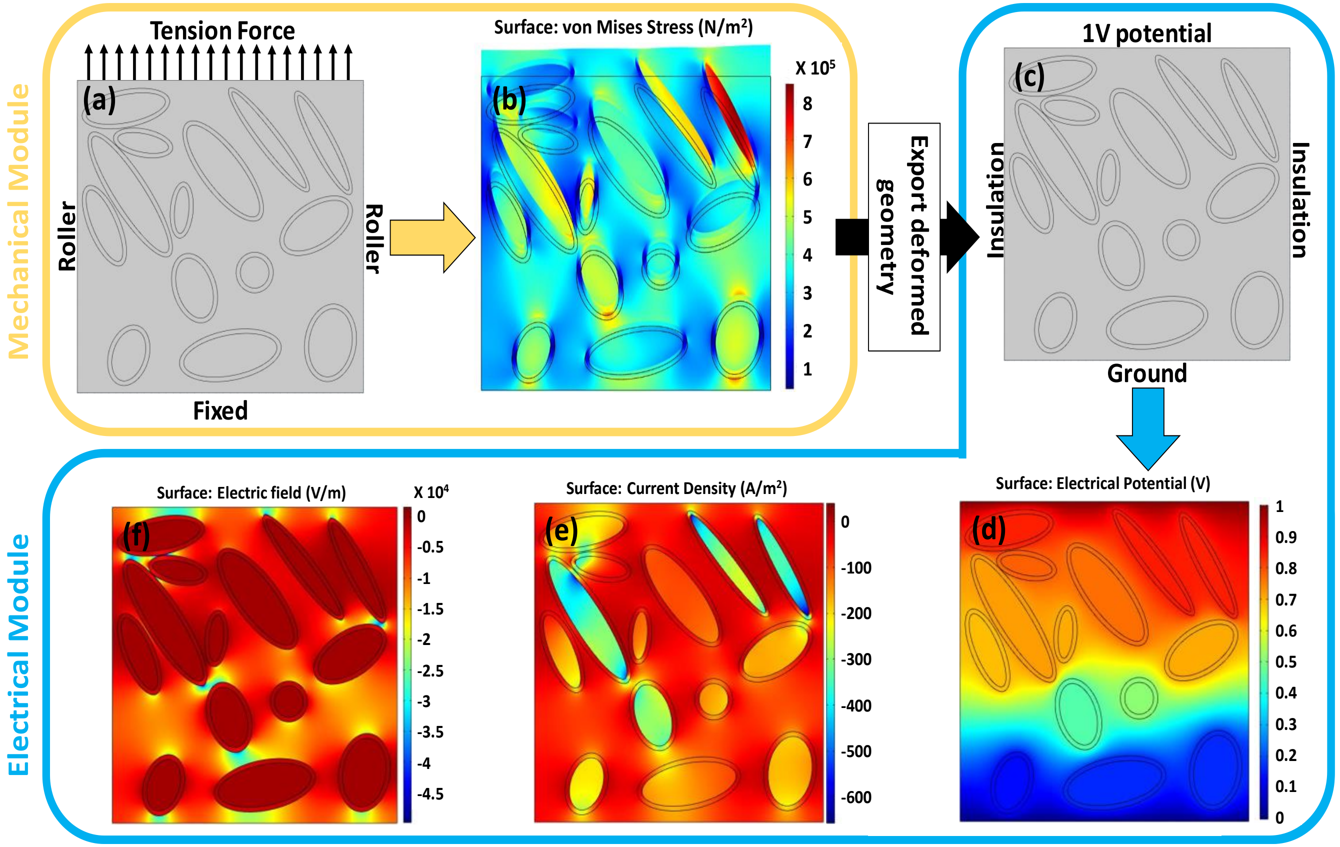

Phases	ε	σ (S/m)	σ_∞ (S/m)	ε_∞	ε_0	τ (s)	c	m	s
Matrix	Eq. 5	Eq. 6	0.002	20	1.25 x 10^7	0.02	0.80	0.99	0.01
Interface			0.008	50	6 x 10^7	0.0086	0.40		
Inclusion	3	100	--						

- Simulated frequency of 100 Hz (the frequency at which conductivity asymptotes)
- Area averaged complex conductivity from current density and the electric field: $\sigma = \frac{<J>}{<E>}$
- composite conductivity generally invariant at frequencies >100 Hz - the asymptotic magnitude of conductivity used to calculate bulk resistance
- $\frac{\Delta R}{R_0} = \frac{\sigma_0}{\sigma} - 1$

Interfacial debonding

Arizona State University

- Mismatch is due to discontinuities in the microstructure from the imposed mechanical loading - produces spurious electric fields and current density under imposed electrical potential
- Effects of interfacial debonding
- Debonding at the paste-inclusion interface captured using cohesive zone modeling
- Debonding considered to occur when the initiation criterion for Mode I fracture is satisfied – i.e., the stress equals the cohesive strength
- Tensile Strength (f'_t), tensile energy release rate (G_{IC}), and stress intensity factor (K_{IC}) from companion experiments available

Electro-mechanical FE modeling with debonding

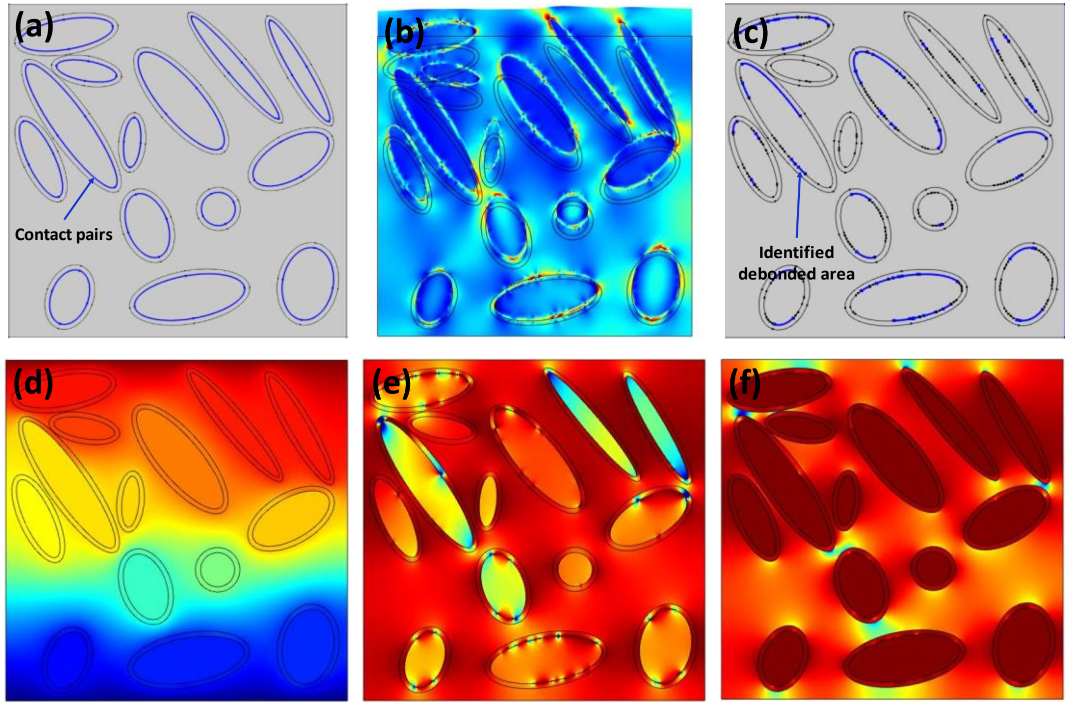

- Contact pairs created at the intersection of the interface and inclusion
- Traction-separation law adopted to describe the mechanical behavior of these contact pairs
- Consideration of tolerance in the models to account for debonding (pseudo thickness of the debonded zone)
- FE meshing for the electrical model much finer than that for the mechanical model, to ensure convergence

Predictions

- Simulations were carried out at three different frequencies – 100 Hz, 1 kHz, and 100 kHz.
- Simulated fractional changes in resistance are found to be frequency independent (within the range considered)
- Model captures strain sensing adequately even when the traction-separation relations are invariant of the inclusion dosage
- Accounting for debonding is a significant requirement

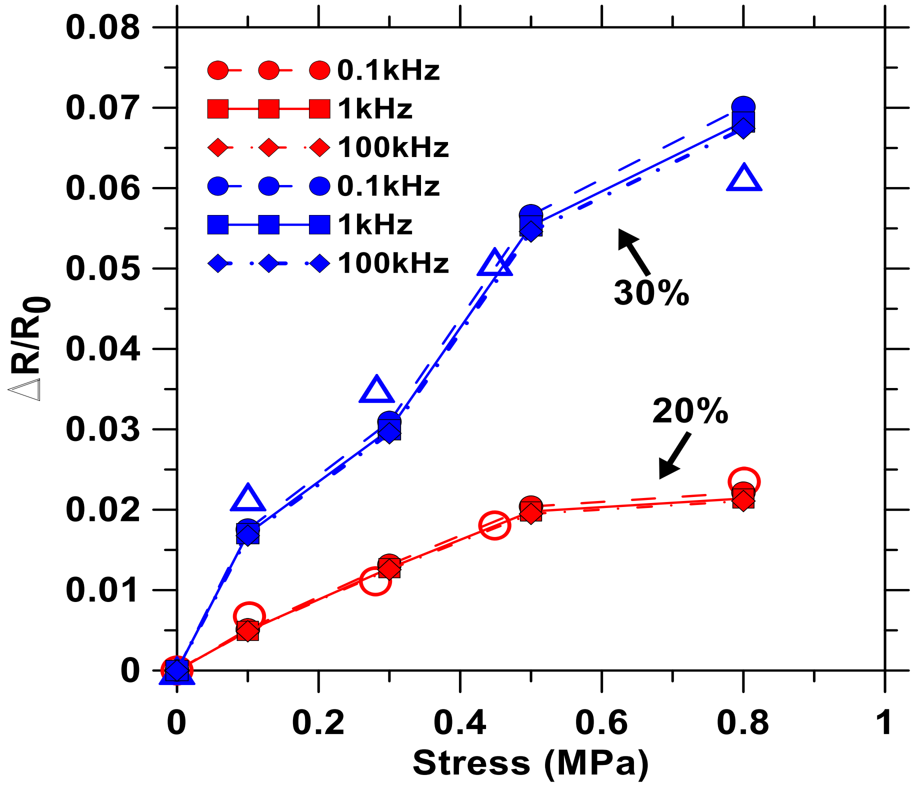

Conclusions

- 0-40% by volume of particulates; mechanical properties rather constant
- Electrical impedance spectroscopy (EIS) and circuit modeling was used to determine the composite resistances
- Gage factor (ratio of fractional resistance to strain), an indicator of strain sensing efficiency, comparable to those of pastes containing small volume fractions of carbon nanofibers or other more expensive conductive inclusions
- Simplified material microstructure accounting for all the phases, and frequency-dependent electrical properties derived from experimental results helps predict $\Delta R/R$
- Interfacial debonding through contact pairs ensured realistic current flow under load
- Modeling methodology generic enough to be applied for different heterogeneous microstructures – can be used to guide self-sensing composite development

This work was funded by the National Science Foundation

Thank you

Narayanan.Neithalath@asu.edu